Closed-Form Least-Squares Source Location Estimation from Range-Difference Measurements

JULIUS O. SMITH, MEMBER, IEEE, AND JONATHAN S. ABEL, MEMBER, IEEE

Abstract—**Three noniterative techniques are presented for localizing a single source given a set of noisy range-difference measurements. The localization formulas are derived from *linear* least-squares "equation error" minimization, and in one case the maximum likelihood bearing estimate is approached. Geometric interpretations of the equation error norms minimized by the three methods are given, and the statistical performances of the three methods are compared via computer simulation.**

I. INTRODUCTION

THE problem of automatically locating a radiating or reflecting source by analyzing signals received from the object is a basic one having numerous applications in navigation, surveillence, aerospace, and geophysics. This paper presents and compares computationally efficient solutions to the problems of locating point sources in constant velocity media using measurements from passive, stationary sensor arrays.

Signals propagating from the source arrive at the sensors of the array at times dependent on the source-sensor geometry and medium characteristics. Differences in arrival times of source signals seen among the sensors of the array are measurable in many cases [1], [13], [14], and can be used to infer the location of a source [1], [2]. In a constant velocity medium, these *time differences of arrival* (TDOA's) are proportional to differences in source-sensor range, termed *range differences* (RD's). The source location is conventionally found as the weighted intersection of the set of hyperboloids (locus of constant-RD source positions for each RD) defined by the RD measurements, a computation which can be quite cumbersome and expensive.

An extensive literature exists on the problem of estimating RD's from received signals [13]. Additionally, much effort has been put into defining and describing properties of optimal passive location estimates [7]–[12]. Few papers, however, address the explicit calculation of the source location estimators [3]–[6], [9]. For a general multisource, multisensor geometry, Wax and Kailath [11] derive an expression for the likelihood function, and give the *maximum likelihood* (ML) source location estimate as its maximizer (found by using an appropriately initialized gradient descent method). Hahn [9] considers the two-dimensional problem of estimating the range and bearing of a source using a line array, and gives closed-form expressions for the maximum likelihood source location estimator for the case of the source far from the sensor array. Carter [10] (see also [8], [7], and [12]) also considers the problem of optimally estimating the range and bearing of an acoustic source using a line array. He presents the ML range and bearing estimates as maximizers of the power seen at the output of a processing system whose configuration is determined by hypothesized source range and bearing; no explicit method for computing the optimal range and bearing is given, however. In the general case, Schmidt [3] has proposed a formulation in which the source location is found as a focus of a conic specified by the sensor locations and RD measurements. Schmidt's method can be extended to a closed-form localization technique which we consider in this paper. In [4], a gradient search localization procedure is proposed for computing optimal source locations from noisy RD's. In [6], a formula is given for single-source RD localization from four sensors, and an extended version of this algorithm is also considered here.

This paper introduces a new closed-form localization technique, termed the *spherical-interpolation (SI) method*. The SI method is similar in formulation to a method of Schau and Robinson [6] which we call the *spherical-intersection (SX) method*. Simulation results are presented in which the SI method shows about an order of magnitude greater noise immunity than the SX method. We compare the SI method also to a third closed-form localization technique, called the *plane-intersection (PX) method*. The PX method is quickly derived from certain formulas due to Schmidt [3]. In Monte-Carlo simulations, the PX method shows approximately a factor of four greater variance than the SI method, although slightly less bias.

This paper is organized as follows. In Section II we derive the SI method for closed-form localization of a single source in a field of N sensors. Next, the SX and PX methods are briefly described. In Section III, simulation results are presented for two different source locations and two additive RD noise levels. Section IV gives a geometric interpretation of all three techniques, and Section V is a discussion.

Manuscript received March 24, 1986; revised June 11, 1987.
The authors are with Systems Control Technology, Palo Alto, CA 94303.
IEEE Log Number 8716988.

II. Closed-Form Localization from Range-Difference Measurements

Let N denote the number of sensors, and let d_{ij} denote the RD between sensors i and j ($i, j = 1, \cdots, N$). The vector of (x, y, z) spatial coordinates for the ith sensor is denoted $\underline{x}_i$, and the position of the source is denoted $\underline{x}_s$. The *distance* between the source and sensor i is denoted by $D_i = \|\underline{x}_i - \underline{x}_s\|$, and the distance from the origin to the point x_i is denoted R_i. Similarly, $R_s = \|\underline{x}_s\|$. These quantities appear in Fig. 1(a).

We have the following basic relation:

$$d_{ij} \triangleq D_i - D_j, \qquad i = 1, \cdots, N, \quad j = 1, \cdots, N. \tag{1}$$

The localization problem is to determine $\underline{x}_s$ given d_{ij} for i and j between 1 and N. Note that there are

$$\binom{N}{2} = \frac{N(N-1)}{2}$$

distinct RD's d_{ij} (excluding $i = j$, and counting each $d_{ij} \equiv -d_{ji}$ pair once). However, in the noiseless case, any $N - 1$ RD measurements which form a "minimal spanning subtree" determine all the rest. The redundancy of the complete set of RD's is used to increase noise immunity (an optimal technique is given in [18]).

It is desired to estimate the source location as the one which, in some sense, best fits the measured RD's. The L_2 norm of the vector difference between the measured range differences and those given by a hypothesized source location is a natural choice for a goodness-of-fit criterion. Under suitable assumptions, its minimizer is seen to be the *maximum likelihood* estimate (cf. Section IV). However, it is a nonconvex function of the source location, and serious difficulties occur in computing its minimizer. In the sequel we shall see that the source localization problem can be solved in closed form by picking the source location as the minimizer of the norm of a so-called "equation error," i.e., the minimizer of the difference between values of *functions* of the measured range differences and *functions* of a hypothesized source location.

A. The Equation-Error Formulation

We first map the spatial origin to an arbitrary sensor, say the jth. This gives

$$\underline{x}_j \triangleq \underline{0} \Rightarrow \begin{cases} R_j = 0 \\ D_j = R_s. \end{cases} \tag{2}$$

From the Pythagorean theorem and (2) in (1), we have

$$(R_s + d_{ij})^2 = R_i^2 - 2\underline{x}_i^T\underline{x}_s + R_s^2 \tag{3}$$

and

$$0 = R_i^2 - d_{ij}^2 - 2R_s d_{ij} - 2\underline{x}_i^T\underline{x}_s \tag{4}$$

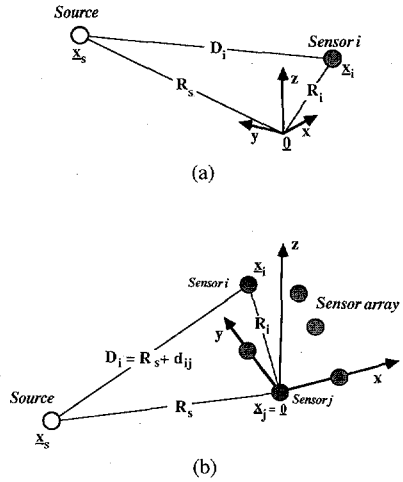

Fig. 1. Diagram illustrating notation and certain geometric relations. Labels imbedded within a line denote the length of the corresponding vector. For example, $D_i = \|\underline{x}_i - \underline{x}_s\|$.

as illustrated in Fig. 1(b). We consider instances of (4) involving the $N - 1$ RD's measured relative to sensor j; so we have $N - 1$ equations in three unknowns $\underline{x}_s$.

As the delays are typically not measured precisely, we introduced a so-called "equation error" [16] into the left-hand side of (4), and minimize it in a least-squares sense to provide an estimate of the true solution. Without loss of generality, let $j = 1$. Then (4) becomes

$$\epsilon_i = R_i^2 - d_{i1}^2 - 2R_s d_{i1} - 2\underline{x}_i^T\underline{x}_s, \qquad i = 2, 3, \cdots, N \tag{5}$$

where ϵ_i is the equation error to be minimized. The set of $N - 1$ equations (5) can be written in matrix notation as

$$\underline{\epsilon} = \underline{\delta} - 2R_s\underline{d} - 2S\underline{x}_s \tag{6}$$

where

$$\underline{\delta} \triangleq \begin{bmatrix} R_2^2 - d_{21}^2 \\ R_3^2 - d_{31}^2 \\ \vdots \\ R_N^2 - d_{N1}^2 \end{bmatrix}, \qquad \underline{d} \triangleq \begin{bmatrix} d_{21} \\ d_{31} \\ \vdots \\ d_{N1} \end{bmatrix},$$

$$S \triangleq \begin{bmatrix} x_2 & y_2 & z_2 \\ x_3 & y_3 & z_3 \\ \vdots & \vdots & \vdots \\ x_N & y_N & z_N \end{bmatrix}.$$

It is worth noting that the equation error vector (6) is *linear in $\underline{x}_s$ given R_s*, and it is *linear in R_s given $\underline{x}_s$*. Error vectors which are linear in the unknowns yield closed-form least-squares solutions.

The formal least-squares solution for $\underline{x}_s$ *given* R_s is

$$\underline{x}_s = \tfrac{1}{2}S_W^*(\underline{\delta} - 2R_s\underline{d}) \tag{7}$$

where

$$S_W^* \triangleq (S^T S)^{-1} S^T \tag{8}$$

yields the minimizer of $\underline{\epsilon}^T \underline{\epsilon}$. If it is desired to weight the RD's according to *a priori* confidence in each RD, then the *weighted equation error* energy $\underline{\epsilon}^T \boldsymbol{W} \underline{\epsilon}$ is minimized for

$$S_W^* \triangleq (S^T W S)^{-1} S^T W \tag{9}$$

where $\boldsymbol{W}$ is a symmetric positive definite (or simply diagonal and positive).

The source range R_s is not typically known *a priori*, and to obtain the x_s minimizing $\underline{\epsilon}^T \boldsymbol{W} \underline{\epsilon}$, it is necessary to allow R_s to vary, maintaining the relation $R_s = \|\underline{x}_s\|$. This, unfortunately, is a difficult nonlinear minimization problem. However, in this case, the nonlinearity can be *approximately* eliminated as described in the next section.

B. The Spherical-Interpolation Method

The basic idea of the new closed-form solution is to substitute (7) into (6) and minimize the equation error again, this time with respect to R_s. This, surprisingly, yields a linear least-squares problem for finding R_s, and the solution is simple and inexpensive. The technique is made possible by the fact that the formal least-squares estimate of $\underline{x}_s$ given R_s in (6) is itself linear in R_s. When the minimizing R_s value is found in this new linear equation, the corresponding value of $\underline{x}_s$ [via (7)] is automatically a minimizer of the squared equation-error norm with respect to $\underline{x}_s$ given this R_s.

Rewriting the equation error (6) to eliminate $\underline{x}_s$ by substituting the value from (7), we get a new equation error $\underline{\epsilon}'$ which is *linear* in R_s.

$$\begin{aligned}\underline{\epsilon}' &= \underline{\delta} - 2R_s\underline{d} - SS_W^*(\underline{\delta} - 2R_s\underline{d}) \\ &= (\boldsymbol{I} - SS_W^*)(\underline{\delta} - 2R_s\underline{d})\end{aligned}$$

where $\boldsymbol{I}$ is the identity matrix. Define the $N-1$ by $N-1$ symmetric matrices

$$\begin{aligned}\boldsymbol{P}_S &\triangleq SS_W^* = S(S^T W S)^{-1} S^T W \\ \boldsymbol{P}_S^\perp &\triangleq \boldsymbol{I} - \boldsymbol{P}_S.\end{aligned}$$

Note, $\boldsymbol{P}_S$ is a rank 3 *projection* matrix, removing components orthogonal to the space spanned by the columns of $\boldsymbol{S}$. Consequently, $\boldsymbol{P}_S$ is *idempotent* ($\boldsymbol{P}_S^2 = \boldsymbol{P}_S$). Finally, $\boldsymbol{P}_S^\perp$ is an idempotent projection matrix which removes components in the space spanned by the columns of $\boldsymbol{S}$.

In the four-sensor case (the three-RD case), $\boldsymbol{P}_S = \boldsymbol{I}$, and the equation error $\underline{\epsilon}'$ is zero for all choices of R_s. In this case, the proposed method cannot be used to estimate the source range and will give a source location estimate with one degree of ambiguity [see (7)]. In the more general case of N sensors,

$$\underline{\epsilon}' = \boldsymbol{P}_S^\perp(\underline{\delta} - 2R_s\underline{d}) \tag{10}$$

so that

$$\underline{\epsilon}'^T \boldsymbol{V} \underline{\epsilon}' = (\underline{\delta} - 2R_s\underline{d})^T \boldsymbol{P}_S^\perp \boldsymbol{V} \boldsymbol{P}_S^\perp (\underline{\delta} - 2R_s\underline{d}).$$

Minimizing with respect to R_s is a form of *weighted least squares* in which the weighting matrix $\boldsymbol{P}_S^\perp \boldsymbol{V} \boldsymbol{P}_S^\perp$ is of rank $N-4$. The three missing dimensions reflect the degrees of freedom removed by substituting in the least-squares solution (7) for the three spatial source coordinates. (As shown in [5], the missing degrees of freedom represent a projection of (6) orthogonal to the term $S\underline{x}_s$.) The solution is given by

$$\tilde{R}_s = \frac{\underline{d}^T \boldsymbol{P}_S^\perp \boldsymbol{V} \boldsymbol{P}_S^\perp \underline{\delta}}{2\underline{d}^T \boldsymbol{P}_S^\perp \boldsymbol{V} \boldsymbol{P}_S^\perp \underline{d}}. \tag{11}$$

Substituting this solution into (7) yields the source location estimate

$$\begin{aligned}\hat{\underline{x}}_s &= \frac{1}{2} S_W^*(\underline{\delta} - 2\tilde{R}_s\underline{d}) \\ &= \frac{1}{2}(S^T W S)^{-1} S^T W \left(\boldsymbol{I} - \frac{\underline{d}\underline{d}^T \boldsymbol{P}_S^\perp \boldsymbol{V} \boldsymbol{P}_S^\perp}{\underline{d}^T \boldsymbol{P}_S^\perp \boldsymbol{V} \boldsymbol{P}_S^\perp \underline{d}}\right)\underline{\delta}.\end{aligned} \tag{12}$$

Defining $\boldsymbol{P}_{\underline{d}}^\perp \triangleq \boldsymbol{I} - \underline{d}\,\underline{d}^T/(\underline{d}^T\underline{d})$, it can be shown [5], [17] that when $\boldsymbol{V} = \boldsymbol{W}$, the estimator (12) is the minimizer of

$$J_{\underline{x}_s} = \underline{\epsilon}^T \boldsymbol{P}_{\underline{d}}^\perp \boldsymbol{W} \boldsymbol{P}_{\underline{d}}^\perp \underline{\epsilon}, \tag{13}$$

a weighted norm of the *projected* equation error (6). Minimizing $J_{\underline{x}_s}$, one gets an expression equivalent to (12) [17]:

$$\hat{\underline{x}}_s = \tfrac{1}{2}(S^T \boldsymbol{P}_{\underline{d}}^\perp \boldsymbol{W} \boldsymbol{P}_{\underline{d}}^\perp S)^{-1} S^T \boldsymbol{P}_{\underline{d}}^\perp \boldsymbol{W} \boldsymbol{P}_{\underline{d}}^\perp \underline{\delta}. \tag{14}$$

Clearly, the computational burden of (12) is very low compared to iterative nonlinear minimization. If iterative nonlinear minimization is desired (to obtain the lowest possible variance and bias), (12) provides an excellent initial value for a general descent method.

Note that, in general, $\tilde{R}_s$ as computed by (11) is not necessarily equal to $\|\underline{x}_s\|$ computed from (12), except as the RD noise approaches zero. Therefore, we define the *range estimate* by

$$\hat{R}_s \triangleq \|\hat{\underline{x}}_s\|$$

instead of using (11). Similarly, the *bearing estimate* is defined as the vector of direction cosines from the origin at sensor 1 to the source:

$$\hat{\underline{\Omega}}_s \triangleq \frac{\hat{\underline{x}}_s}{\hat{R}_s} = \frac{\hat{\underline{x}}_s}{\|\hat{\underline{x}}_s\|}. \tag{15}$$

C. The Spherical-Intersection Method

The SX solution [6] is obtained by substituting the least-squares solution (7) for $\underline{x}_s$ given R_s into the quadratic equation $R_s^2 = \underline{x}_s^T \underline{x}_s$:

$$R_s^2 = [\tfrac{1}{2} S_W^*(\underline{\delta} - 2R_s\underline{d})]^T [\tfrac{1}{2} S_W^*(\underline{\delta} - 2R_s\underline{d})]. \tag{16}$$

This yields, after expansion,

$$aR_s^2 + bR_s + c = 0 \tag{17}$$

where

$$a = 4 - 4\underline{d}^T \boldsymbol{S}_W^{*T} \boldsymbol{S}_W^* \underline{d}, \qquad b = 4\underline{d}^T \boldsymbol{S}_W^{*T} \boldsymbol{S}_W^* \underline{\delta},$$
$$c = -\underline{\delta}^T \boldsymbol{S}_W^{*T} \boldsymbol{S}_W^* \underline{\delta}. \tag{18}$$

The two solutions to the quadratic equation (17) are

$$\hat{R}_s = \frac{-b \pm \sqrt{b^2 - 4ac}}{2a}. \tag{19}$$

The positive root is taken as an estimate of the source-to-sensor-1 distance $\hat{R}_s$ [6]. This value of $\hat{R}_s$ is then substituted into (7) to obtain the source location $\underline{\hat{x}}_s$.

D. The Plane-Intersection Method

The method of Schmidt [3] solves the localization problem in a *plane* by forming differences between instances of (3) for three different sensors. The differences are arranged so as to eliminate quadratic terms, leaving only terms linear in $\underline{x}_s$. Since a detailed derivation appears in [3, p. 822], we give only the final result, generalized to three space in the same way [3, p. 834]:

$$\epsilon_{ijk} \triangleq 2\Delta_{ijk}^T \boldsymbol{S}_{ijk} \underline{x}_s - [d_{ji} d_{kj} d_{ik} + R_i^2 d_{kj} + R_j^2 d_{ik} + R_k^2 d_{ji}] \tag{20}$$

where

$$\Delta_{ijk} \triangleq \begin{bmatrix} d_{kj} \\ d_{ik} \\ d_{ji} \end{bmatrix}, \qquad \boldsymbol{S}_{ijk} \triangleq \begin{bmatrix} \underline{x}_i^T \\ \underline{x}_j^T \\ \underline{x}_k^T \end{bmatrix}. \tag{21}$$

Since the equation error ϵ_{ijk} (20) is linear in $\underline{x}_s$, it can be used as the basis of a closed-form solution in a manner analogous to the use of (5). The least-squares solution so obtained will be called the *plane-intersection (PX) method*. Note that the solutions suggested in [3] are not the same.

III. Simulation Results

This section presents simulation results comparing the statistical performance of all three closed-form localizers on the problem of localizing a single source in the presence of noise. The localizers are the SI, SX, PX methods, and the equations for each are (12), (19), and (7), and the unweighted least-squares solution to (20), respectively. The three localization formulas are compared according to the bias and variance of the source location estimate. The results indicate that the SI and PX methods perform comparably (with the SI method exhibiting lower variance), and show much higher noise immunity than the SX method.

All simulations employed the 9-sensor array geometry shown in Fig. 2, with the two source locations shown and two levels of additive white noise in the RD's. The sample bias and variance were obtained by averaging the results of 100-trial Monte-Carlo runs. Each method was run using eight equations and the same set of estimated RD's: d_{i1}, $i = 2, \cdots, 9$. The eight equations used in the PX method used RD's from this set two at a time, involving sensors (1, 2, 3), (1, 3, 4), $\cdots$, (1, 8, 9), and (1, 9, 2). Our simulated range-difference estimates were generated by adding white Gaussian noise to true RD values.

Table I describes the environmental information (source location, range, bearing, and additive noise level) or each of four 100-trial Monte-Carlo runs (two source locations and two RD noise levels). The sensor locations are (0, 0, 0) (0, 0, 100) (0, 0, 200) (100, 0, 0) (100, 0, 100) (100, 0, 200) (0, 100, 0) (0, 100, 100) (0, 100, 200).

Table II shows the *sample bias* for each Monte-Carlo run, listing errors in the Euclidean 3-D source coordinates and errors in range and bearing. The bearing error is computed in degrees as

$$\theta_s - \hat{\theta}_s \triangleq \frac{180}{\pi} \cos^{-1} (\hat{\underline{\Omega}}_s^T \underline{\Omega}_s).$$

We find that the SI and PX methods have comparable bias, and the SX method has noticeably larger sample bias.

Table III shows the *sample standard deviations* for each Monte-Carlo run, again for both Euclidean and plane-projected polar coordinates. Due to the source-sensor geometry, the bearing is more accurately estimated than the range in all examples; this is typical when the source is several aperture sizes away from the sensor array. The SI method is seen to have the lowest deviation, the PX method about double that of SI, and the SX method deviation is widely varying—from 1.5 to hundreds of times greater than that of the SI method. The estimate variances of the SI and PX methods appear to increase linearly with an increase in RD variance, while the SX method variance increases much faster. At this point, it seems clear that the SX method can be dropped from further consideration.

The relative merits of SI versus PX depend on the relative importance of bias versus standard deviation. One commonly used figure of merit for biased estimators is the *root-mean-squared (rms) error*, defined by

$$\bar{\sigma} \triangleq \sqrt{\text{bias}^2 + \text{variance}}. \tag{22}$$

This performance measure is listed in Table IV. For this source-sensor configuration, we see that when squared bias and variance are rated equally, the SI method is the superior technique; the SI method has much reduced variance and only slightly higher bias than the PX method. In Monte-Carlo results not presented here, using various different source locations, sensor geometries, and levels of additive noise, the SI method was seen to have the lower sample rms error than the other methods in every case.

The extent to which the minimizer of $\underline{\epsilon}^T \boldsymbol{P}_{\underline{d}}^{\perp} \boldsymbol{W} \boldsymbol{P}_{\underline{d}}^{\perp} \underline{\epsilon}$ [the

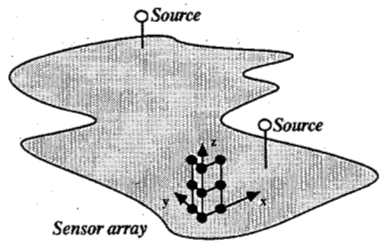

Fig. 2. Source-sensor geometry used in the Monte-Carlo simulations.

TABLE I
ENVIRONMENTAL INFORMATION FOR THE FOUR SIMULATION CASES

Run 1—Source location $\underline{x}_s$: (390, 160, 170)
Range R_s: 454.5
Bearing cosines $\underline{\Omega}_s$: (0.858, 0.352, 0.374)
RD noise standard deviation $\sigma_{d_{i1}} = 0.1$

Run 2—Source location $\underline{x}_s$: (390, 160, 170)
Range R_ss: 454.4
Bearing cosines $\underline{\Omega}_s$: (0.858, 0.352, 0.374)
RD noise standard deviation $\sigma_{d_{i1}} = 1$

Run 3—Source location $\underline{x}_s$: (540, 1360, 110)
Range R_s: 1467
Bearing cosines $\underline{\Omega}_s$: (0.368, 0.927, 0.075)
RD noise standard deviation $\sigma_{d_{i1}} = 0.1$

Run 4—Source location $\underline{x}_s$: (540, 1360, 110)
Range R_s: 1467
Bearing cosines $\underline{\Omega}_s$: (0.368, 0.927, 0.75)
RD noise standard deviation $\sigma_{d_{i1}} = 1$

TABLE II
SAMPLE BIAS MEASUREMENTS, 100 TRIALS

Method	Run	Source Location Bias $\hat{x}_s - x_s$	$\hat{y}_s - y_s$	$\hat{z}_s - z_s$	Range $\hat{R}_s - R_s$	Bearing $\hat{\theta}_s - \theta_s$
Spherical Interpolation	1	0.239	0.60	0.026	0.225	0.010
	2	5.16	1.47	0.837	5.42	0.174
	3	1.87	4.60	0.003	4.95	0.014
	4	62.7	165	1.40	178	0.500
Plane Intersection	1	0.195	0.052	−0.035	0.183	0.010
	2	4.24	1.22	0.602	4.19	0.150
	3	0.961	2.18	−0.035	2.37	0.009
	4	26.9	72.5	1.8	76.9	0.2
Spherical Intersection	1	0.341	0.090	0.048	0.341	0.012
	2	0.316	−0.129	−0.057	0.129	0.035
	3	−2.00	−5.76	−0.090	−6.10	0.017
	4	−585 $+22i$	−1597 $+60i$	−13.9 $+0.5i$	1700 $+63i$	8.3 $+7.9i$

SI method, cf, (13)] is different from the minimizer of $\underline{\epsilon}^T \boldsymbol{W} \underline{\epsilon}$ (the desired solution) is indicated by the extent to which $\tilde{R}_s$ computed by (11) is not equal to $\|\underline{\hat{x}}_s\|$ computed by (12). It was therefore of interest to compare these quantities. In the high-noise case above ($\sigma_{d_{i1}} = 1$), for both source positions, the quantity $|1 - \|\underline{\hat{x}}_s\|/\tilde{R}_s|$ was typically less than 0.005 and almost never greater than 0.01. Thus, the SI method is very close to the desired least-squares equation-error minimizer under the above conditions. It would be of interest to determine under what conditions, if any, the SI method is significantly different from the minimizer of $\underline{\epsilon}^T \boldsymbol{W} \underline{\epsilon}$.

IV. GEOMETRIC INTERPRETATION

This section gives geometric interpretations of the three closed-form solutions and discusses them in light of the Monte-Carlo results presented above. These geometric models help interpret the effects of noisy RD measure-

TABLE III
SAMPLE STANDARD DEVIATION MEASUREMENTS, 100 TRIALS

Method	Run	Source Location Error $\sigma_{\hat{x}_s}$	$\sigma_{\hat{y}_s}$	$\sigma_{\hat{z}_s}$	Range $\sigma_{\hat{R}_s}$	Bearing $\sigma_{\hat{\theta}_s}$
Spherical Interpolation	1	2.07	0.698	0.445	2.27	0.042
	2	20.4	6.91	4.39	22.4	0.41
	3	9.98	26.2	0.600	28.2	0.07
	4	82	219	5	234	0.7
Plane Intersection	1	4.17	1.33	0.898	4.37	0.07
	2	40.3	12.8	8.732	42.2	0.66
	3	15.8	42.5	0.817	45.2	0.11
	4	159	421	7	449	1
Spherical Intersection	1	3.12	1.10	0.513	3.24	0.066
	2	31.1	11.1	5.13	32.4	0.64
	3	39.4	105	0.958	112	0.28
	4	5854 $+159i$	15914 $+412i$	126 $+0i$	16956 $+14i$	25 $+24i$

TABLE IV
SAMPLE RMS ERROR MEASUREMENTS, 100 TRIALS

Method	Run	Source Location Error $\bar{\sigma}_{\hat{x}_s}$	$\bar{\sigma}_{\hat{y}_s}$	$\bar{\sigma}_{\hat{z}_s}$	Range $\bar{\sigma}_{\hat{R}_s}$	Bearing $\bar{\sigma}_{\hat{\theta}_s}$
Spherical Interpolation	1	2.08	0.700	0.446	2.28	0.043
	2	21	7.06	4.47	23	0.45
	3	10.1	26.6	0.600	28.6	0.071
	4	103	274	5.2	294	0.7
Plane Intersection	1	4.18	1.33	0.898	4.37	0.07
	2	40.5	12.9	8.75	42.4	0.68
	3	15.8	42.6	0.818	45.3	0.11
	4	161	427	7	456	1
Spherical Intersection	1	3.12	1.1	0.515	3.25	0.067
	2	31.1	11.1	5.13	32.4	0.64
	3	39.4	105	0.962	112	0.28
	4	5855	15999	127	17041	37

ments on the resulting solution, and suggest how the methods will perform in various source-sensor geometries.

A. The Error Criterion

The goal is to localize the source $\underline{x}_s$ and therefore to minimize $\|\underline{x}_s - \hat{\underline{x}}_s\|$ for some norm. We will only consider the L_2 (sum-of-squares) norm. Since we are given measurements $\underline{d}$, the best formulation would appear to be

$$\min_{\underline{x}_s} \|\underline{\epsilon}^*\| \triangleq \|\underline{d} - \hat{\underline{d}}(\underline{x}_s)\| \tag{23}$$

where $\underline{d}$ is the vector of measured RD's, and $\hat{\underline{d}}(\underline{x}_s)$ is the vector of RD's corresponding to the hypothesized source location $\underline{x}_s$. This error criterion is especially well suited to the case of zero-mean errors in the RD's. Indeed, if the RD errors are independent Gaussian perturbations, then (23) provides the *maximum likelihood estimate* for $\hat{\underline{x}}_s$ (which is now regarded as a parameter determining the mean $\hat{\underline{d}}(\hat{\underline{x}}_s)$ of the multivariate normal distribution for $\underline{d}$). For this reason, the solution to (23) will be referred to as the maximum likelihood estimate of the source location.

Placing sensor 1 at the origin as before (in the case of only d_{i1}, $i = 1, \cdots, N$ available), (23) can be interpreted as finding the sphere, passing through (that is, *interpolating*) sensor 1, whose surface is as close as possible to being d_{i1} away from the ith sensor. This arrangement is shown in Fig. 3 for the noiseless case.

As seen in Fig. 4, the sphere of radius $\hat{R}_s$, centered at $\hat{\underline{x}}_s$ and passing through sensor 1, is a surface of zero RD to sensor 1. The distance from the sphere to sensor i is $\hat{d}_{i1}$. The problem is then to position $\hat{\underline{x}}_s$ such that $\hat{d}_{i1} \approx d_{i1}$ for every i. Accordingly, the error minimized in (23) is equivalent to the sum of squared differences between the sphere-to-sensor distance $\hat{d}_{i1}$ and the measured RD d_{i1} for the sensor.

As mentioned in the introduction, solving (23) requires costly nonlinear minimization techniques. For this rea-

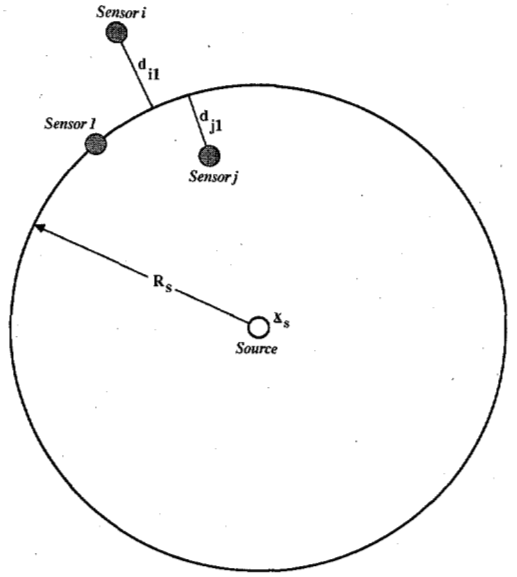

Fig. 3. The spherical interpolation interpretation of the sensor array, source, and RD geometry. The sphere of radius R_s drawn around the source is the surface of zero RD relative to sensor 1. The perpendicular distance from the sphere to any sensor is the RD for the sensor relative to sensor 1.

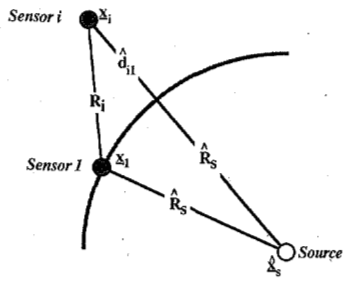

Fig. 4. Geometric representation of the relationship given in (5).

son, none of the closed-form solutions discussed in this paper solves (23). Instead, they minimize (or approximately minimize) the L_2 norm of an "equation error" which was chosen purely to simplify the solution. As seen in the Monte-Carlo results, some errors yield better minimizers than others.

B. Spherical Interpolation

We first show that the equation error (5) (approximately minimized by the SI method) is closely related to the maximum likelihood error minimized in (23). Adding and subtracting R_s^2 in the definition of the equation error (5) gives (upon introducing hats to denote estimated quantities)

$$\begin{aligned}\epsilon_i &= R_i^2 - 2\underline{x}_i^T\hat{\underline{x}}_s + \hat{R}_s^2 - (d_{i1}^2 + 2\hat{R}_s d_{i1} + \hat{R}_s^2) \\ &\qquad i = 2, 3, \cdots, N \\ &= \|\underline{x}_i - \hat{\underline{x}}_s\|^2 - (\hat{R}_s + d_{i1})^2 \qquad (24)\end{aligned}$$

where $\hat{\underline{x}}_s$ and $\hat{R}_s$ are the estimated source location and range, $\underline{x}_i$ is the ith sensor location (known exactly), and d_{i1} is the measured range difference. Let

$$\hat{d}_{i1} = \|\underline{x}_i - \hat{\underline{x}}_s\| - \hat{R}_s$$

denote the RD predicted by the source location estimate $\hat{\underline{x}}_s$ (cf. Fig. 4). Then (24) can be written as

$$\begin{aligned}\epsilon_i &= (\hat{R}_s + \hat{d}_{i1})^2 - (\hat{R}_s + d_{i1})^2 \\ &= 2\hat{R}_s(d_{i1} - \hat{d}_{i1}) + d_{i1}^2 - \hat{d}_{i1}^2 \\ &= (d_{i1} + \hat{d}_{i1} + 2\hat{R}_s)(d_{i1} - \hat{d}_{i1}). \qquad (25)\end{aligned}$$

Assuming that the noise in the delay estimates is small compared to the intersensor spacing, ϵ_i is well approximated by

$$\begin{aligned}\epsilon_i &\approx 2(\hat{R}_s + \hat{d}_{i1})(d_{i1} - \hat{d}_{i1}) \\ &= 2\,\hat{D}_i\,(d_{i1} - \hat{d}_{i1}).\end{aligned}$$

This form of the error displays the equation error as the maximum likelihood error $d_{i1} - \hat{d}_{i1}$ times the source-sensor distance estimate. When the source range is large compared to the intersensor separation, the SI equation error reduces to

$$\epsilon_i \approx 2\hat{R}_s(d_{i1} - \hat{d}_{i1}).$$

The difference between the SI method and the maximum likelihood method is the tendency of the SI solution to pull the estimated source location *toward the origin*, thereby making $\hat{R}_s$ and the equation error smaller. This contraction of the source estimate toward sensor 1 was consistently observed in the simulations. Note that there is no difference between the maximum likelihood solution and the SI method with respect to *bearing estimation* when $R_s >> |d_{i1}| + |\hat{d}_{i1}|$.

The above discussion leads naturally to a weighting function and an iterative technique for obtaining the solution to (23). The weighting matrix $\boldsymbol{W}$ in (9) should be given by

$$\boldsymbol{W} = (\text{diag}\,[\hat{D}_i]\,\boldsymbol{R}_{\underline{d}}\,\text{diag}\,[\hat{D}_i])^{-1} \qquad (26)$$

where diag (x_i) is a diagonal matrix with x_i as the ith row/column element, $\boldsymbol{R}_{\underline{d}}$ is the RD measurement correlation matrix, and $\hat{D}_i$ is given by a prior solution of (5), or estimated from *a priori* information. The solution of (23) is then found by iteratively solving (5) with successively updated values of $\boldsymbol{W}$ using (26). If this iteration converges (it may not), then the weighting cancels the first term of (25) and the maximum likelihood error remains. It should be emphasized that conditions for convergence to the solution of (23) need to be determined.

C. Spherical Intersection

The SX method finds the source location as the intersection of spheres of radius $d_{i1} + \hat{R}_s$ drawn around each sensor (see Fig. 5) [6]. This method has some inherent instabilities (also shown in Fig. 5). When the source is not close to the sensor array, the spheres have relatively large radii, and any error in RD estimation can show up as a large error in source location estimate. Because of

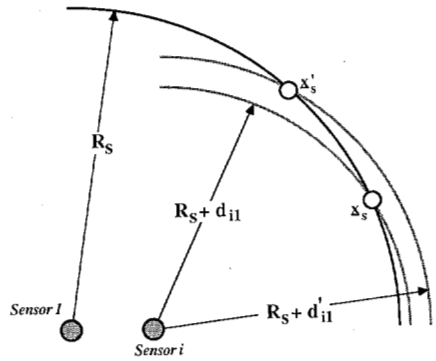

Fig. 5. The SX method. Circles of radius $R_s + d_{i1}$ are intersected to form an estimate of the source location.

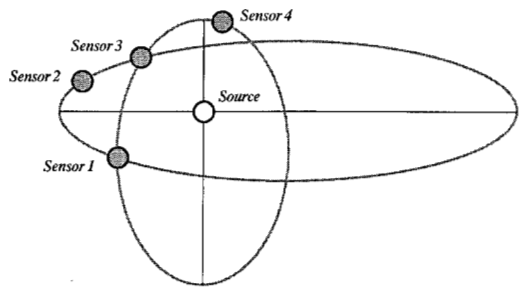

Fig. 6. The geometry of the PX method. Equations are formed using RD's from a sensor triplet to define line through the foci of a conic. The source, which lies at one of the foci, is found by the least-squares intersection of such lines.

this, it is suggested that the SX method be used only when the source is close to the array, or when the RD's are known precisely.

D. Plane Intersection

The PX method employs intersecting planes. Each set of 3 sensors and RD measurements defines a plane on which the source lies. Planes resulting from RD measurements among different sets of sensors are intersected to obtain a source location estimate.

On each plane lies a conic whose surface contains the 3 sensors. The source is located at one of the foci of the conic (see Fig. 6). In [3], planes are constructed which pass through the foci of these conics. These equations are relatively simple to write in terms of the RD's of the sensor triplet, and are linear in the source coordinates.

From a geometric point of view, it is not clear to us why the SI method should have consistently lower variance and slightly higher bias than the PX method. Perhaps it can be shown that the error minimized by the SI method is closer to the maximum likelihood error than is the one minimized by the PX method.

V. Discussion

The problem of localizing a source given a set of measured RD's from an N-sensor array was considered, and three closed-form source location estimators were presented. These estimators represent a tremendous computational savings over the exhaustive search methods required to compute the optimal (ML) estimate as the maximizer of a nonconvex function. If ML performance is desired, the estimators will provide excellent starting points for gradient-based *iterative* maximizing of the likelihood function.

Monte-Carlo simulations were used to compare the statistical performance of the closed-form estimators. It was found that the SI method exhibited the lowest rms error. The SI estimate is to be closely related to the maximum likelihood estimate for the case of Gaussian RD measurement errors.

The estimators are minimizers of weighted equation error norms. The equation errors were developed to be linear in the source location, and the localization formulas are derived using standard linear least-squares methods. The formulation of an error linear in the source location allows *standard* Kalman filters rather than *extended* Kalman filters to be used in tracking moving sources [15], [17].

Finally, a note on multisource localization. In the presence of M uncorrelated sources, there will be M RD's seen in each sensor pair—one for each source. The localization problem is therefore to associate the measured RD's with their originating sources, and to localize each source based on its RD measurements. The association of the range differences with their sources must be done by searching over all possible associations, looking for the one with the most self-consistency (i.e., the association giving the minimum, for some norm, of the difference between the measured RD's and those predicted by source locations estimated based on the assumed association). This computation typically involves $O(M^{N-1})$ conversions of RD values into source location estimates, and is feasible with the computationally efficient closed-form solutions provided here.

Acknowledgment

The authors would like to thank the reviewers for helpful comments and several references.

References

[1] P. M. Janiczek, Ed., *Global Positioning System*. Washington, DC: The Institute of Navigation, 1980.

[2] J. P. Van Etten, "Navigation systems: Fundamentals of low and very low frequency hyperbolic techniques," *Electric. Commun.*, vol. 45, no. 3, pp. 192–212, 1970.

[3] R. O. Schmidt, "A new approach to geometry of range difference location," *IEEE Trans. Aerosp. Electron.*, vol. AES-8, pp. 821–835, Nov. 1972.

[4] J. M. Delosme, M. Morf, and B. Friedlander, "A linear equation approach to locating sources from time-difference-of-arrival measurements," in *Proc. IEEE Int. Conf. Acoust., Speech, Signal Processing*, 1980.

[5] J. S. Abel and J. O. Smith, "The spherical interpolation method for closed-form passive source localization using range difference measurements," in *Proc. IEEE Int. Conf. Acoust., Speech, Signal Processing*, 1987.

[6] H. C. Schau and A. Z. Robinson, "Passive source localization employing intersecting spherical surfaces from time-of-arrival differences," *IEEE Trans. Acoust., Speech, Signal Processing*, vol. ASSP-35, pp. 1223–1225, Aug. 1987.

[7] V. H. MacDonald and P. M. Schultheiss, "Optimum passive bearing

estimation," *J. Acoust. Soc. Amer.*, vol. 46, no. 1, pp. 37–43, Oct. 1969.

[8] W. J. Bangs and P. M. Schultheiss, "Space-time signal processing for optimal parameter estimation," in *Signal Processing*, J. W. R. Griffiths, P. L. Stocklin, and C. van Schooneveld, Eds. New York: Academic, 1973, pp. 577–590.

[9] W. R. Hahn, "Optimum signal processing for passive sonar range and bearing estimation," *J. Acoust. Soc. Amer.*, vol. 58, no. 1, pp. 201–207, July 1975.

[10] G. C. Carter, "Variance bounds for passively locating an acoustic source with a symmetric line array," *J. Acoust. Soc. Amer.*, vol. 62, no. 4, pp. 922–926, Oct. 1977.

[11] M. Wax and T. Kailath, "Optimum localization of multiple sources in passive array," *IEEE Trans. Acoust., Speech, Signal Processing*, vol. ASSP-31, pp. 1210–1217, Oct. 1983.

[12] L. C. Ng, "Optimum multisensor, multitarget localization and tracking," Ph.D. dissertation, Univ. Conn., Storrs, 1983.

[13] Special Issue on Time-Delay Estimation, *IEEE Trans. Acoust., Speech, Signal Processing*, vol. ASSP-29, June 1981.

[14] B. Friedlander, "On the Cramer–Rao bound for time delay and Doppler estimation," *IEEE Trans. Inform. Theory*, vol. IT-30, pp. 575–580, May 1984.

[15] R. L. Moose and T. E. Dailey, "Adaptive underwater target tracking using passive multipath time-delay measurements," *IEEE Trans. Acoust., Speech, Signal Processing*, vol. ASSP-33, pp. 777–786, Aug. 1985.

[16] L. Ljung and T. Soderstrom, *Theory and Practice of Recursive Identification*. Cambridge, MA: M.I.T. Press, 1984.

[17] B. Friedlander, "A passive localization algorithm and its accuracy analysis," *IEEE J. Ocean. Eng.*, vol. OE-12, pp. 234–245, Jan. 1987.

[18] W. R. Hahn and S. A. Tretter, "Optimum processing for delay-vector estimation in passive arrays," *IEEE Trans. Inform. Theory*, vol. IT-12, pp. 608–614, Sept. 1973.

Julius O. Smith (M'76) was born in Memphis, TN, on March 6, 1953. He received the B.S.E.E. degree from Rice University, Houston, TX, in 1975. He received the M.S. and Ph.D. degrees from Stanford University, Stanford, CA, in 1978 and 1983, respectively, on a Hertz Foundation Graduate Fellowship.

From 1975 to 1977 he worked in the Signal Processing Department at ESL, Sunnyvale, CA, on systems for digital communications. From 1982 to 1986 he was with the Adaptive Systems Department of Systems Control Technology, Palo Alto, CA, where he worked in the areas of adaptive filtering and spectrum estimation. He is presently employed at NeXT, Inc., developing signal processing functions for the NeXT personal computer.

Dr. Smith is a member of Tau Beta Pi and Sigma Xi.

Jonathan S. Abel (M'85) was born in Sarasota, FL, in December 1960. He received the S.B. degree in electrical engineering from the Massachusetts Institute of Technology, Cambridge, in 1982, and won the 1982 Guilleman Award for his thesis work on conducting polymers. He received the M.S. degree in electrical engineering from Stanford University, Stanford, CA, in 1984, where he is currently a Ph.D. candidate in the Information Systems Laboratory

He joined Systems Control Technology, Palo Alto, CA, in 1985 as a Research Engineer in the Advanced Technology Division, where he has been working in the areas of signal processing and statistics.